ORIGINAL ARTICLE

Targeting of TAM Receptors Ameliorates Fibrotic Mechanisms in Idiopathic Pulmonary Fibrosis

Milena S. Espindola[1]*, David M. Habiel[1]*, Rohan Narayanan[1], Isabelle Jones[1], Ana L. Coelho[1], Lynne A. Murray[2], Dianhua Jiang[1], Paul W. Noble[1], and Cory M. Hogaboam[1]

[1]Department of Medicine, Cedars-Sinai Medical Center, Los Angeles, California; and [2]Respiratory, Inflammation and Autoimmunity, MedImmune Ltd., Cambridge, United Kingdom

Abstract

Rationale: Idiopathic pulmonary fibrosis (IPF) is characterized by aberrant lung remodeling, which progressively abolishes lung function in an RTK (receptor tyrosine kinase)–dependent manner. Gas6 (growth arrest–specific 6) ligand, Tyro3 (TYRO3 protein tyrosine kinase 3), and Axl (anexelekto) RTK expression and activity are increased in IPF.

Objectives: To determine if targeting these RTK pathways would inhibit fibroblast activation and the development of pulmonary fibrosis.

Methods: Quantitative genomic, proteomic, and functional analyses were used to determine Gas6/TAM (Tyro3, Axl, and Mertk [MER proto-oncogene, tyrosine kinase]) RTK expression and activation in tissues and fibroblasts from normal and IPF lungs. The profibrotic impact of these RTK pathways were also examined in bleomycin-induced pulmonary fibrosis and in SCID/Bg mice that developed pulmonary fibrosis after the intravenous administration of primary IPF fibroblasts.

Measurements and Main Results: Gas6, Axl, and Tyro3 were increased in both rapidly and slowly progressive IPF compared with normal lung samples and fibroblasts. Targeting these pathways with either specific antibodies directed at Gas6 or Axl, or with small-molecule TAM inhibitors indicated that the small molecule–mediated targeting approach was more efficacious in both *in vitro* and *in vivo* studies. Specifically, the TAM receptor inhibitor R428 (also known as BGB324) significantly inhibited the synthetic, migratory, and proliferative properties of IPF fibroblasts compared with the other Gas6/TAM receptor targeting agents. Finally, loss of Gas6 expression decreased lung fibrotic responses to bleomycin and treatment with R428 inhibited pulmonary fibrosis in humanized SCID/Bg mice.

Conclusions: Gas6/TAM receptor activity contributes to the activation of pulmonary fibroblasts in IPF, suggesting that targeting this RTK pathway might be an effective antifibrotic strategy in this disease.

Keywords: IPF; TAM receptors; lung fibrosis; Axl; fibroblasts

At a Glance Commentary

Scientific Knowledge on the Subject: Gas6 (growth arrest–specific 6) and TAM (Tyro3 [TYRO3 protein tyrosine kinase 3], Axl [anexelekto], and Mertk [MER proto-oncogene, tyrosine kinase]) receptor tyrosine kinases promote both the synthetic and invasive properties of primary human idiopathic pulmonary fibrosis fibroblasts. Targeting of Tyro3, Axl, and Mertk receptors blocks the profibrotic effect of these cells in various tissue culture assays and in immunodeficient mice.

What This Study Adds to the Field: Tyro3, Axl, and Mertk receptor kinases are putative targets in the treatment of idiopathic pulmonary fibrosis.

(Received in original form July 27, 2017; accepted in final form April 6, 2018)

*These authors contributed equally.

Supported by Cedars-Sinai Medical Center and an NIH R01 grant (HL123899; Cedars-Sinai Medical Center).

Author Contributions: Conception and design, M.S.E., D.M.H., R.N., I.J., D.J., P.W.N., and C.M.H. Acquisition of data, M.S.E., D.M.H., R.N., I.J., L.A.M., and A.L.C. Analysis and interpretation of data, M.S.E., D.M.H., and C.M.H. Drafting the manuscript and intellectual content, M.S.E., D.M.H., and C.M.H.

Correspondence and requests for reprints should be addressed to Cory M. Hogaboam, Ph.D., Women's Guild Lung Institute, Department of Medicine, Cedars-Sinai Medical Center, Los Angeles, CA, 90048. E-mail: cory.hogaboam@cshs.org.

This article has an online supplement, which is accessible from this issue's table of contents at www.atsjournals.org.

Am J Respir Crit Care Med Vol 197, Iss 11, pp 1443–1456, Jun 1, 2018
Copyright © 2018 by the American Thoracic Society
Originally Published in Press as DOI: 10.1164/rccm.201707-1519OC on April 10, 2018
Internet address: www.atsjournals.org

Idiopathic pulmonary fibrosis (IPF) is a lethal lung disease with a poorer prognosis than many cancers (1). The Food and Drug Administration approval of nintedanib/BIBF1120 for the treatment of IPF in 2014 confirmed the utility of targeting RTKs (receptor tyrosine kinases) in the treatment in this disease. Nintedanib targets multiple RTKs but its primary targets include platelet-derived growth factor receptors, vascular endothelial growth factor receptors, and fibroblast growth factor receptors (2, 3). The antifibrotic effects of nintedanib have increased enthusiasm for the exploration of the role of RTKs in IPF.

For example, the Gas6 (growth arrest–specific 6)/TAM (Tyro3 [TYRO3 protein tyrosine kinase 3], Axl [anexelekto], and Mertk [MER proto-oncogene, tyrosine kinase]) receptor pathway seems to have a role in organ remodeling. Gas6 is a secreted ligand that was identified in growth-arrested embryonic mouse NIH 3T3 fibroblasts (4). However, Gas6 is actually a pleotrophic growth factor that rescues serum-deprived cells from apoptosis, and it regulates cell differentiation in several adult cell types (5). Gas6 binds to all three TAM receptors, but its highest affinity is for Axl. TAM receptors activate multiple signaling pathways responsible for cell survival, growth, differentiation, adhesion, and motility, including NF-κB (nuclear factor-κB), PI3k (phosphoinositide 3-kinase), Akt (also known as protein kinase B), STAT3 (signal transducer and activator of transcription 3), and Ras/ERK (extracellular signal-regulated kinase) (6). Several stimuli induce the expression of both Gas6 and Axl, including various TLR (Toll-like receptor) ligands, T-helper cell type 2 cytokines, IFN-α, vitamin K, TGF (transforming growth factor)-β, and reactive oxygen species (4, 7). A role for TAM receptors in stromal cell activation has been previously demonstrated (8, 9) due in part to the regulation of TGF-β (10). *In vivo*, Gas6 promotes peribronchial fibrosis in allergic airway disease (11, 12) and the genetic absence of Gas6 has been shown to prevent liver inflammation and fibrosis in mice (13). Although Gas6 has emerged as a clinically relevant biomarker of liver fibrosis (14) and targeting this mediator is a promising therapeutic strategy in this disease (15–17), the role of Gas6/TAM receptors has not been investigated previously in IPF.

The aim of the present study was to investigate the expression and role of Gas6/TAM receptors in IPF via the analysis of lung tissues, primary fibroblasts, mesenchymal $SSEA4^+$ progenitors derived from these tissues, and murine models of pulmonary fibrosis. Expression of Gas6/TAM receptor pathway components is increased and active in IPF and experimental pulmonary fibrosis. Importantly, the TAM receptor antagonist R428 (also known as BGB324) effectively and consistently targeted fibrotic mechanisms both *in vitro* and *in vivo*.

Methods

Patients and Study Approval

Clinical characteristics of the patients with IPF were published previously (18, 19). Institutional review boards both at the University of Michigan (Hum00004350) and at Cedars-Sinai Medical Center (Pro34067 and Pro00035396) approved all experiments. All patients were consented before inclusion in these studies.

Human Cells and Cell Culture Conditions

Primary lung fibroblasts were generated by dissociation of lung biopsies or explants and cultured in complete media (Dulbecco's modified Eagle medium [Lonza] containing 15% fetal bovine serum [Atlas Biologicals], 100 IU penicillin and 100 μg/ml streptomycin [Lonza], 292 μg/ml L-glutamine [Lonza], and 100 μg/ml of Primocin [Invivogen]) at 37°C and 10% CO_2. A total of 29 primary human fibroblast lines (i.e., 16 IPF and 13 normal lines) and five primary $SSEA4^+$ progenitor cell lines were examined, and 0.5×10^4 cells/well or 2.5×10^5 cells/well were plated onto a 96- or six-well plates, respectively. Cells were incubated overnight, then washed and treated with the antibodies or small-molecule inhibitors: S6-1 or S6-2 (4 μg/ml; Aravive Biologics), anti-Axl (20 μg/ml; Genentech), or IgG (20 μg/ml; Biolegend); TAM receptor small-molecule inhibitors R428 (2 or 10 μM; Selleckchem), LDC1267 (LDC; 5 or 25 μM; Selleckchem); or nintedanib (also referred to as BIBF1120 or BIBF, 300 nM; Boehringer Ingelheim). Inhibitor-treated cells were also exposed to CpG (10 μM; Hycult Biotech) or TGF-β (20 ng/ml; R&D Systems) and further analyzed (*see* the online supplement).

Mouse Models of Fibrosis

Six- to 8-week-old female C.B-17SCID/beige mutation (SCID/Bg) mice (Jackson Laboratories) were housed at Cedars-Sinai Medical Center. C57BL/6J (Jackson Laboratories) and $Gas6^{-/-}$ (20) mice were bred at the University of Michigan Unit for Laboratory Animal Medicine. For the experiments performed in SCID/Bg mice, IPF fibroblasts were cultured in complete media, washed, and resuspended in serum-free medium before intravenous injection of 1×10^6 fibroblasts. Other SCID/bg mice were not injected (i.e., naive). Humanized SCID/Bg mice were treated with R428 (5 mg/kg), BIBF1120 (30 mg/kg), or the appropriate vehicle by oral gavage at 2 hours before fibroblast injection and 5 days a week for 5 weeks thereafter. At Day 35 after fibroblast injection, the experiment was terminated, and the following was collected: BAL fluid and serum for protein analysis, the superior and middle lobes for biochemical hydroxyproline quantification, postcaval lobe for qPCR analysis, and the left lung for histologic analysis. For the bleomycin studies, male and female $Gas6^{+/+}$ or $Gas6^{-/-}$ mice (6–10 wk of age) received bleomycin (0.05 U/mouse; 1.7 U/kg) or saline by intratracheal injection. At conclusion of experiment, lungs were collected for analysis. All mouse studies described herein were approved at both institutions. Refer to the online supplement for additional details.

Statistical Analysis

Analyses were performed using GraphPad Prism version 7.0c (GraphPad Software). Data are means ± SEM and assessed for significance by nonparametric Mann-Whitney *U* test or ANOVA. After overall differences were identified by ANOVA, a Tukey multiple comparison test was used to identify significance. Values of P less than 0.05 were considered significant.

Results

Gas6/Axl Transcript and Activated Axl Protein Expression in IPF Lung Tissue

Both Gas6 (Figure 1A) and Axl (Figure 1B) transcript levels were significantly ($P \leq 0.05$) increased in IPF compared with normal lung samples. Comparison of samples from patients with IPF who showed a slower course of disease progression (slow IPF) with those who exhibited a rapid course of disease progression (as previously defined [19]; rapid IPF) revealed that pAxl expression in the latter group was significantly ($P \leq$

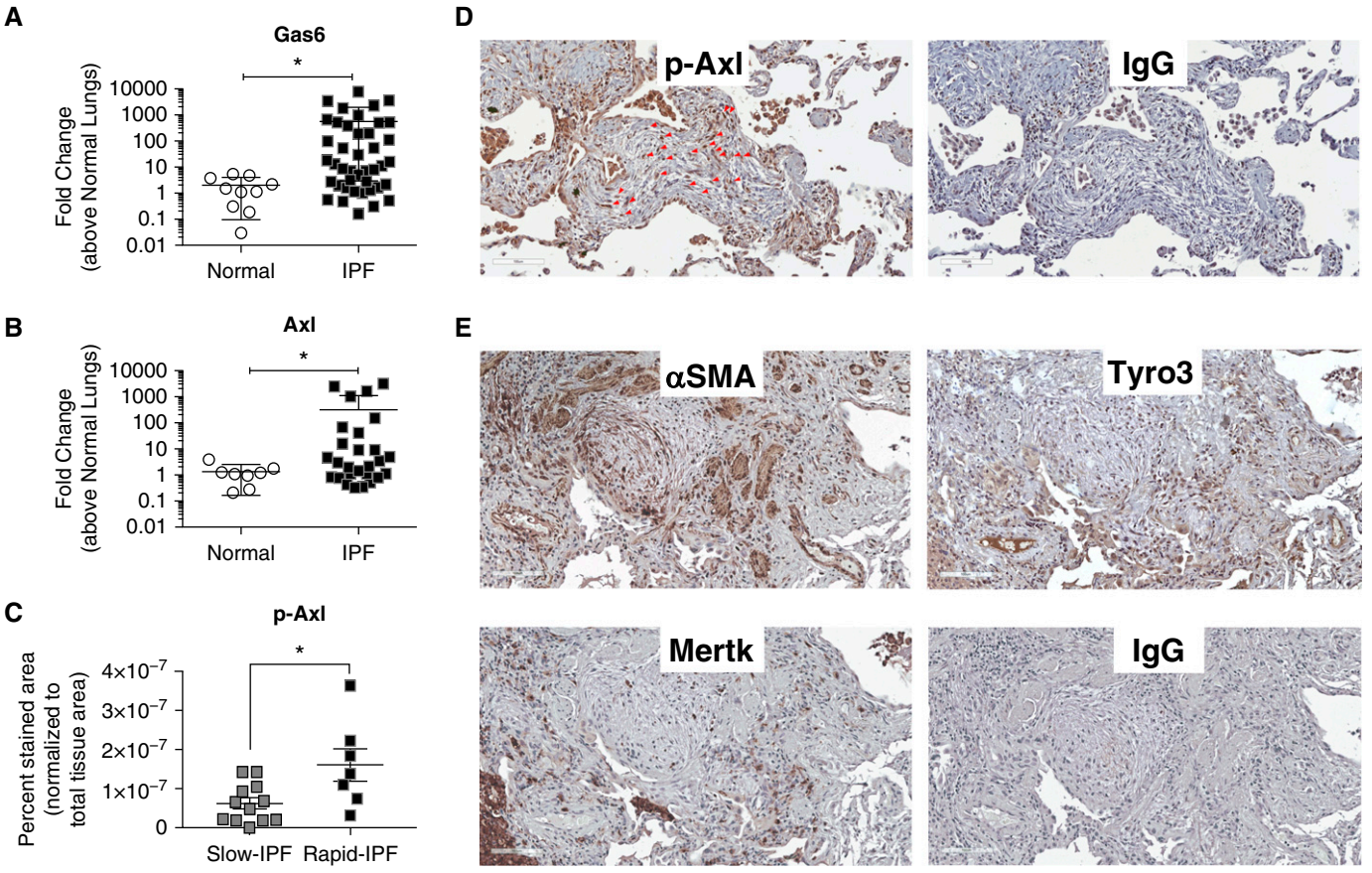

Figure 1. Gas6 and Axl expression and activation in idiopathic pulmonary fibrosis (IPF). (*A* and *B*) Gas6 (*A*) and Axl (*B*) transcript expression were analyzed in surgical lung biopsies from nondiseased patients (normal; $n = 10$) and patients with IPF ($n = 42$) by quantitative PCR. Patients with IPF were stratified as rapid or slow progressors as defined previously (19). (*C*) p-Axl expression was quantified via software analysis (*see* Figure E1) in biopsies from patients with slowly and rapidly progressing IPF. (*D* and *E*) Representative p-Axl, α-smooth muscle actin, Tyro3, and Mertk in contiguous IPF lung sections. IgG control staining for the same areas is shown in both panels. Data in *A* and *B* are mean ± SD and in C mean ± SEM. Scale bars, 100 μm. *$P \leq 0.05$. Red arrows highlight fibroblasts stained for pAxl. α-SMA = α-smooth muscle actin; Axl = anexelekto; Gas6 = growth arrest–specific 6; Mertk = MER proto-oncogene, tyrosine kinase; p-Axl = phosphorylated Axl; Tyro3 = TYRO3 protein tyrosine kinase 3.

0.05) higher than levels detected in the former group (Figure 1C; *see* Figures E1A–E1D and Methods in the online supplement for description of pAxl analysis). As shown in Figure 1D, pAxl protein was detected in fibroblastic foci (red arrows) and other cells in lung biopsy samples from a representative rapid IPF patient. In contiguous lung histologic sections, α-smooth muscle actin (αSMA) and Tyro3 but not Mertk were detected in fibroblastic foci (Figure 1E). In contrast, pAxl was rarely detected in interstitial areas of normal lung, although rare immune cells stained for this phosphorylated receptor (*see* Figures E1E and E1F). Together, these data indicated that Gas6, Axl, and Tyro3 were all elevated in IPF, and p-Axl was present in fibroblastic foci and more abundant in rapid versus slow progressing IPF.

Increased Gas6 Expression and Axl Activation in Primary IPF Fibroblasts and Progenitor Cells

Ingenuity analysis of transcript data from IPF lung biopsies and explants (GSE24206) confirmed that Gas6 was elevated and suggested that several Axl receptor–interacting proteins and downstream mediators associated with this pathway were also elevated (Figures 2A and 2B). RNAseq analysis (GSE103488) of both primary IPF and normal fibroblasts (Figure 2C) and $SSEA4^+$ cells (Figure 2D; described previously by Xia and colleagues [21, 22]) revealed that TAM receptor expression was not different between IPF and normal fibroblasts, whereas Gas6 transcripts were elevated in IPF relative to normal. Ingenuity analysis also indicated that Gas6 and several Axl receptor –interacting proteins and downstream mediators in this pathway were elevated (Figures 2E and 2F). Similar findings were observed in $SSEA4^+$ cells isolated from these two groups of patients with IPF (Figures 2G and 2H). Overall, Gas6 was elevated in IPF fibroblasts and $SSEA4^+$ progenitor cells, and Axl receptor was active in both cell types, particularly in rapid IPF compared with slow IPF.

Selective Targeting of Gas6/Axl with S6 Modulates IPF Fibroblast Activation

As shown in Figure 3A, Axl protein was expressed at similar levels in both normal and IPF fibroblasts. Similar levels of Tyro3 protein were also present in these fibroblasts but weak expression of Mertk protein was observed in two of three normal fibroblast lines but not in any of the IPF fibroblast lines examined

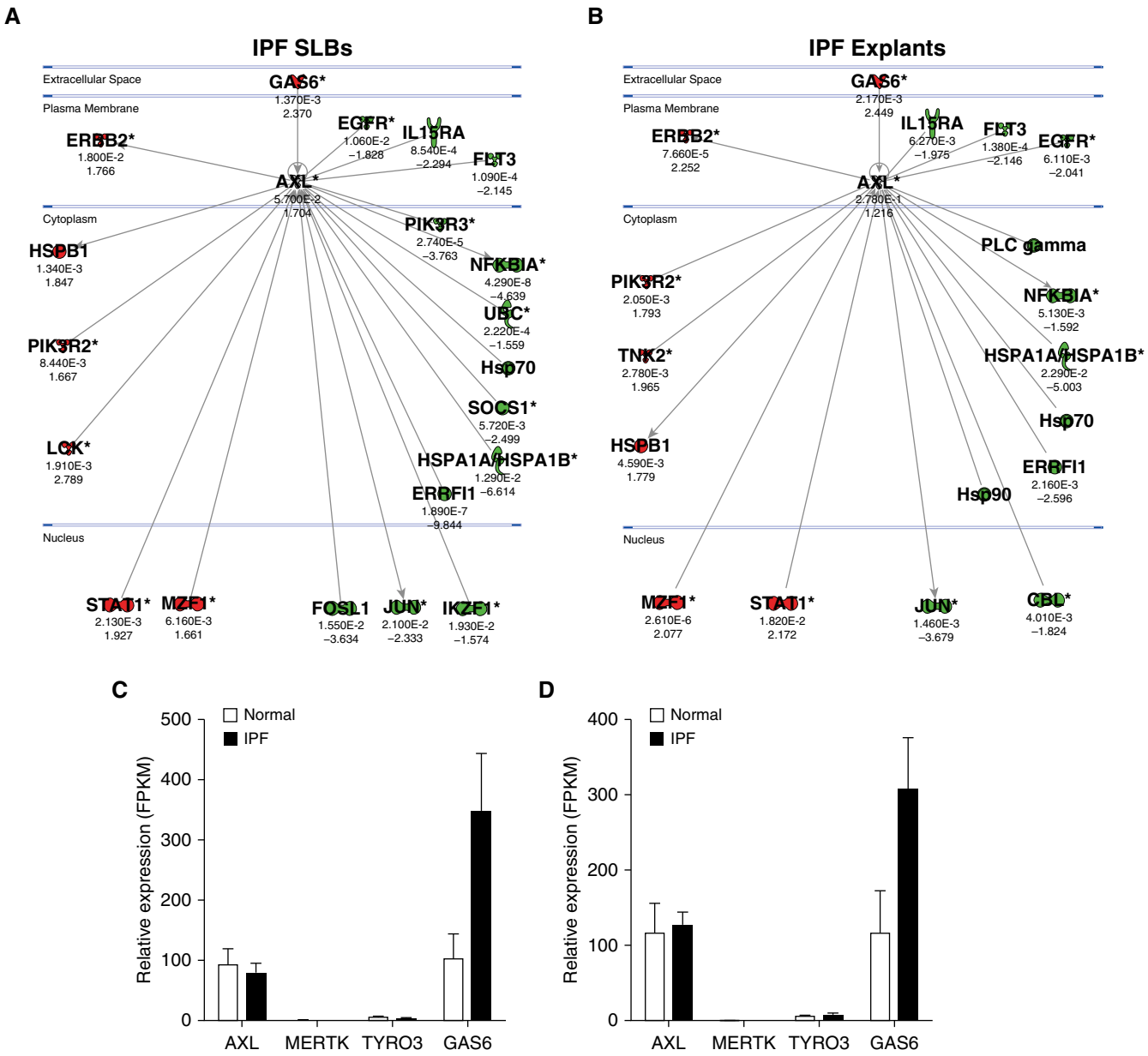

Figure 2. Gas6 and Axl expression in idiopathic pulmonary fibrosis (IPF) fibroblasts and mesenchymal progenitor cells. An Axl interaction network was generated using Ingenuity's knowledge base, and overlaid on relative expression datasets from lung tissue microarray datasets. (*A* and *B*) *P* values (top) and fold change in expression (IPF vs. normal; bottom) from publicly available datasets (GSE24206) comparing IPF surgical lung biopsies (*A*) or IPF explants (*B*) to normal lung tissues. Up- and downregulated transcripts are depicted in red and green, respectively. (*C* and *D*) RNA sequencing was performed on fluorescence-activated cell–sorted SSEA4$^+$ mesenchymal progenitors (*C*) and SSEA4$^-$ fibroblasts (*D*). Average FPKM expression values for Axl, Mertk, Tyro3, and Gas6 from normal ($n = 2$ lines) and IPF ($n = 4$ lines) are shown. Data in *C* and *D* are mean ± SEM. (*E–H*) An Axl interaction network was superimposed over relative expression datasets (GSE103488) from rapid IPF fibroblasts (*E*) ($n = 5$), slow IPF fibroblasts (*F*) ($n = 5$), rapid IPF SSEA4$^+$ cells (*G*) ($n = 5$), and slow IPF SSEA4$^+$ cells (*H*) ($n = 5$). The SSEA4$^+$ cells were sorted from cultures of rapid and slow IPF fibroblasts. Average FPKM values (top) and fold change in expression (IPF vs. normal; bottom) are shown compared with normal equivalent cell types ($n = 3$). Up- and downregulated transcripts are depicted in red and green, respectively. Asterisks denote genes that are represented by multiple probes in microarrays. Axl = anexelekto; FPKM = fragments per kilobase million; Gas6 = growth arrest–specific 6; Mertk = MER proto-oncogene, tyrosine kinase; SLBs = surgical lung biopsies; Tyro3 = TYRO3 protein tyrosine kinase 3.

(Figure 3A). The levels of soluble Axl (i.e., sAxl) were significantly lower in IPF fibroblasts than in similar numbers of normal lung fibroblasts (Figure 3B). We next addressed the targeting of Gas6/Axl using an antibody called S6 (or S6-2), which are recombinant high-affinity soluble Axl decoy receptors (23). Higher free Gas6 levels were present in IPF compared with normal fibroblast cultures but S6 (4 μg/ml) effectively reduced the levels of free Gas6 below the limit of detection in both (Figure 3C). In contrast, BIBF1120 (300 nM) had no effect on the levels of free Gas6 in cultures of human lung fibroblasts (Figure 3D).

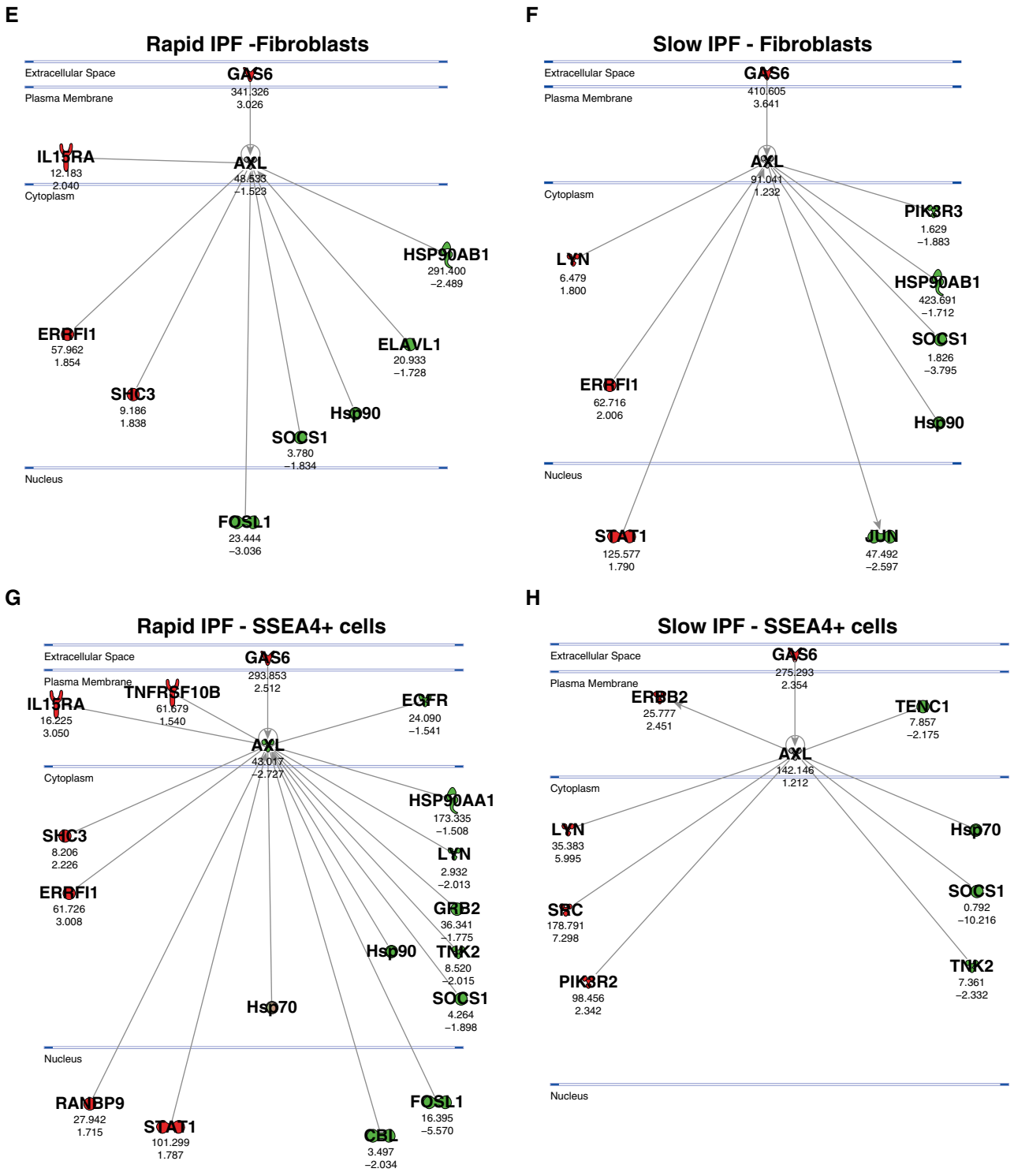

Figure 2. (Continued).

Because we have previously published that hypomethylated CpG-DNA (i.e., CpG) drives IPF myofibroblast differentiation (24), we next determined the role of Gas6/Axl in this process. Although both S6 and BIBF1120 had no effect on constitutive αSMA (dotted line in Figure 3E) expression in normal and IPF fibroblasts, S6 and BIBF1120 significantly attenuated this protein in IPF fibroblasts exposed to CpG compared with control IPF fibroblasts exposed to vehicle and CpG (Figures 3E [quantification, top panel] and 3F [Western blot]). Baseline Axl protein expression in normal and IPF fibroblasts was not altered

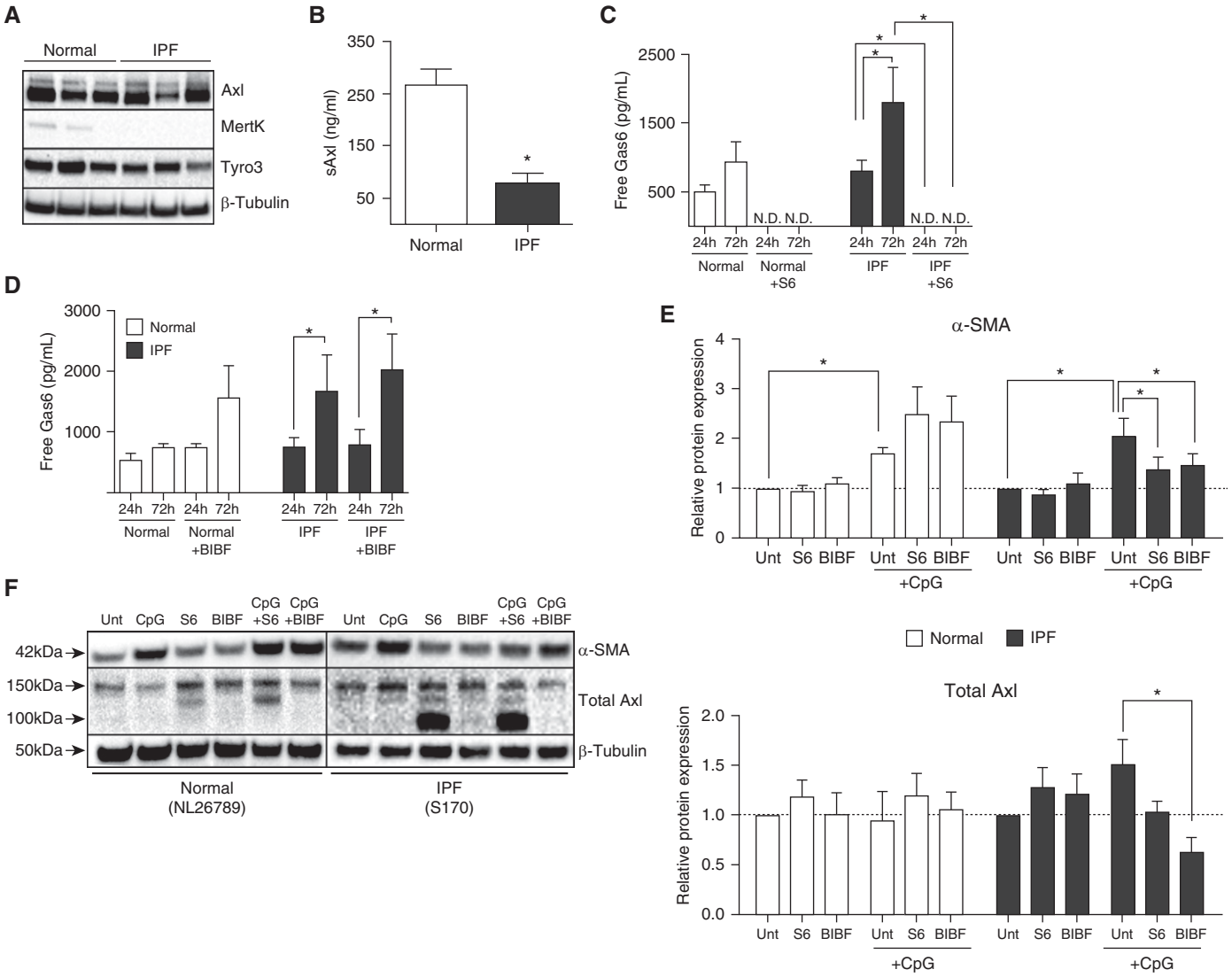

Figure 3. Effects of S6 (a Gas6 decoy receptor) and BIBF1120 on normal and idiopathic pulmonary fibrosis (IPF) myofibroblast differentiation. (*A*) Cultured fibroblasts from normal and IPF lungs were examined by Western blotting for the expression of Axl, Mertk, Tyro3, and β-tubulin. Fibroblasts cultured from normal and IPF lungs were treated with S6 (4 μg/ml), BIBF1120 (300 nM), or vehicle and exposed to CpG (10 μM) for 24 or 72 hours. (*B*) Soluble Axl was measured in untreated fibroblast cultures from normal ($n = 3$) and IPF ($n = 6$) cells lines by ELISA. (*C* and *D*) Free Gas6 was measured by ELISA in normal ($n = 3$) and IPF ($n = 5$) fibroblast cultures treated with S6 (*C*) or BIBF1120 (*D*). (*E*) Western blot analysis of α-SMA and total Axl relative protein expression were quantified from normal ($n = 4$) and IPF ($n = 5$) fibroblast cultures treated with S6 and BIBF1120 in the absence or presence of CpG for 24 hours. Relative protein expression was calculated from ratios of α-SMA or total Axl/β-tubulin, and results were expressed compared with untreated samples. (*F*) Representative blots for α-SMA, total Axl, and β-tubulin. NL26789 and S170 are individual cell lines used in our experiments. Data are mean ± SEM. $^*P \leq 0.05$. α-SMA = α-smooth muscle actin; Axl = anexelekto; BIBF = BIBF1120 (nintedanib); Gas6 = growth arrest–specific 6; Mertk = MER proto-oncogene, tyrosine kinase; N.D. = not detected; sAxl = soluble Axl; Tyro3 = TYRO3 protein tyrosine kinase 3; Unt = untreated.

by S6 or BIBF1120 (Figures 3E [quantification, bottom panel] and 3F [Western blot]) but BIBF1120 significantly reduced total Axl expression in IPF fibroblasts exposed to CpG compared with IPF fibroblasts exposed to the vehicle for this drug and CpG. Together, S6 modulated CpG-induced myofibroblast differentiation via neutralization of Gas6, whereas BIBF1120 modulates the expression of Axl in IPF fibroblasts.

Small-Molecule Inhibitors of TAM Receptors Rather Than Gas6/Axl–Specific Biologics More Effectively Modulate IPF Fibroblast Activation

R428 and LDC are small-molecule inhibitors of TAM receptors (25). We next determined the *in vitro* efficacy of R428 (2 and 10 μM) or LDC (5 μM) compared with BIBF1120 or S6 in normal and IPF fibroblasts. Without the addition of CpG, R428 significantly inhibited pAxl protein levels in cultured IPF and normal fibroblasts, whereas S6 treatment only affected normal fibroblasts compared with the appropriate vehicle control at 1 hour after treatment (Figure 4A). With the addition of CpG, pAxl expression was significantly reduced in R428-treated IPF, but not normal, fibroblasts compared with the vehicle-treated group,

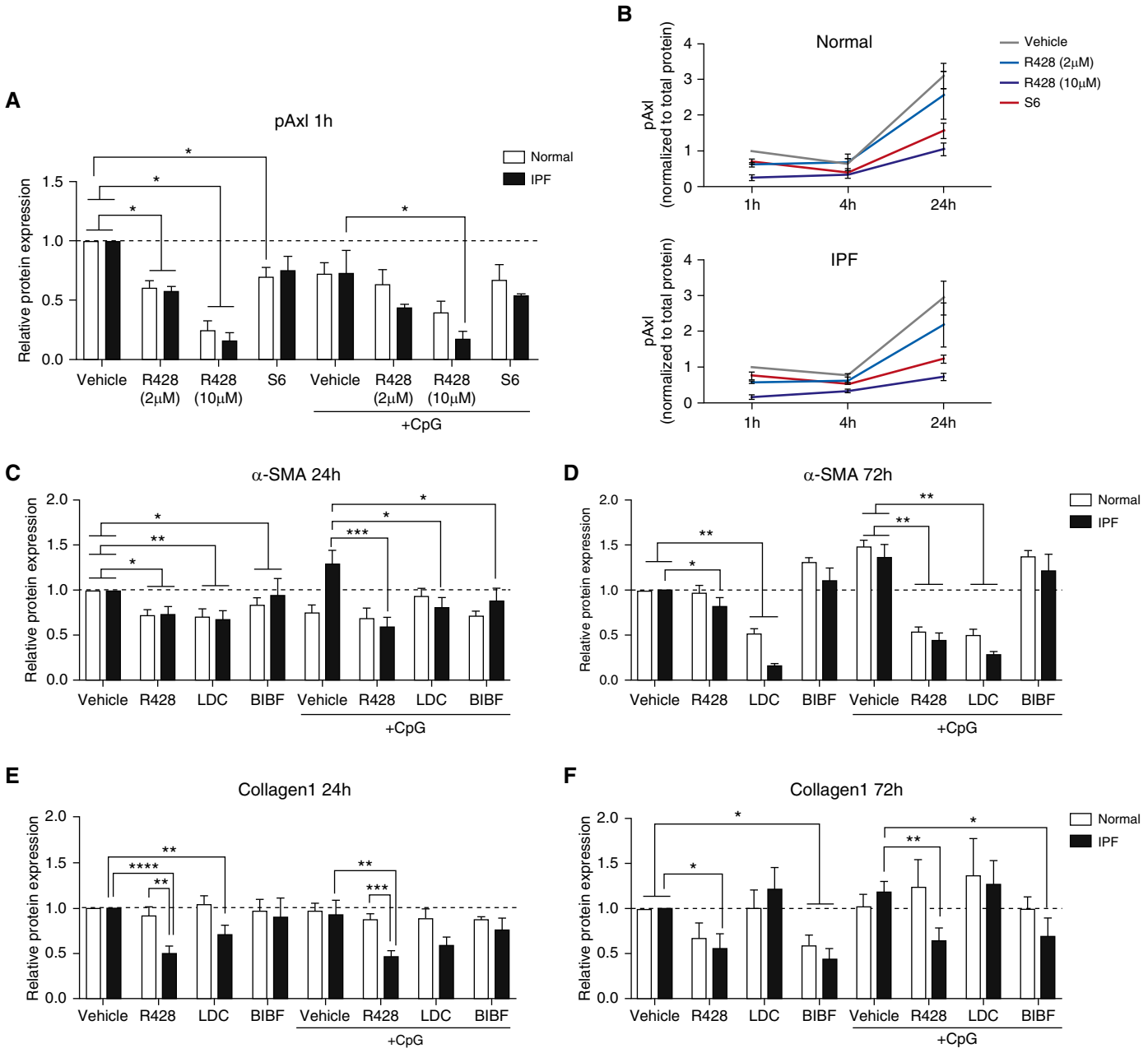

Figure 4. Effects of small molecule TAM (Tyro3, Axl, and Mertk) receptor antagonists and BIBF1120 on normal and IPF myofibroblast differentiation and activation. Fibroblast cultures derived from normal and IPF lung samples were treated with R428 (2 or 10 μM), LDC (5 μM), BIBF1120 (300 nM), S6 (4 μg/ml), or vehicle in the absence or presence of CpG (10 nM) for 1, 4, 24, or 72 hours. (*A* and *B*) Phosphorylated Axl was determined using a PathScan phospho-Axl (panTyr) sandwich ELISA kit, whereas (*C* and *D*) α-SMA was quantified via *in situ* in-cell ELISA and (*E* and *F*) collagen 1 via direct ELISA. Relative protein expression was calculated from ratios of phosphorylated Axl, α-SMA, or collagen 1 to β-tubulin, and results are expressed as fold changes compared with vehicle controls. Data are mean ± SEM, $n = 3$ per group. $^{*}P \leq 0.05$; $^{**}P \leq 0.01$; $^{***}P \leq 0.001$; $^{****}P \leq 0.0001$. α-SMA = α-smooth muscle actin; Axl = anexelekto; BIBF = BIBF1120 (nintedanib); IPF = idiopathic pulmonary fibrosis; LDC = LDC1267; Mertk = MER proto-oncogene, tyrosine kinase; pAxl = phosphorylated Axl; Tyro3 = TYRO3 protein tyrosine kinase 3.

and S6 had a modest effect on pAxl expression (Figure 4A). The inhibitory effect of a 10-μM dose of R428 on pAxl expression was also observed at 4 and 24 hours after R428 treatment in both normal and IPF fibroblasts, whereas S6 showed an apparent inhibitory effect on pAxl expression in normal and IPF fibroblast cultures at 24 hours, albeit to a lesser extent than R428 (Figure 4B).

Both LDC and R428, and to a lesser extent, BIBF1120, had significant inhibitory effects on αSMA expression at 24 hours in normal and IPF fibroblasts with and without CpG compared with the appropriate vehicle control group (Figure 4C). This effect on αSMA expression was persistent for 72 hours in cells treated with LDC and, to a lesser

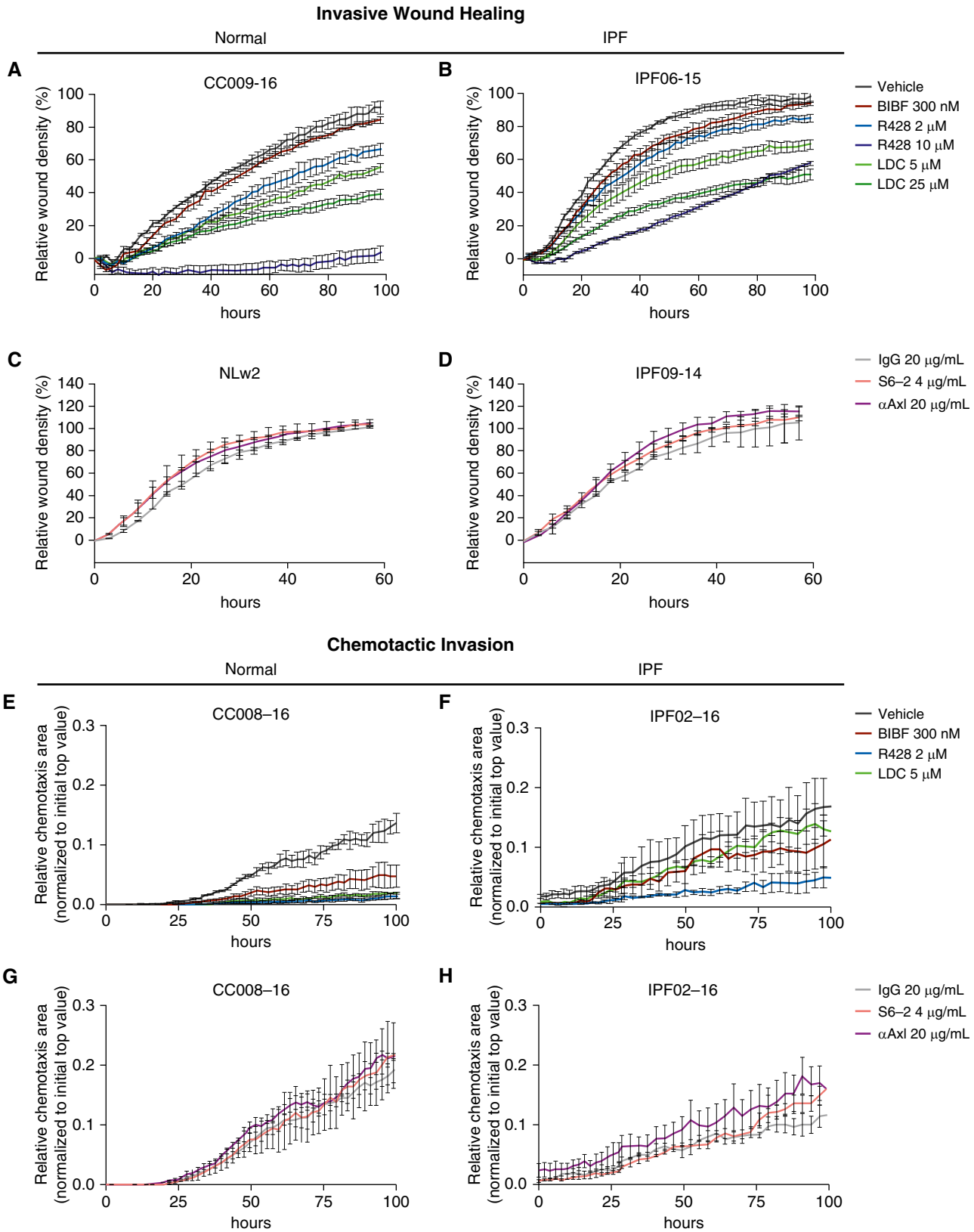

Figure 5. Functional analysis of the role of Gas6/TAM (Tyro3, Axl, and Mertk) receptor activation in normal and IPF fibroblast invasion. Normal and IPF fibroblasts were treated with the small-molecule inhibitors R428 (2 and 10 μM) and LDC (5 and 25 μM); BIBF1120 (300 nM) or vehicle; and the antibodies S6 (4 μg/ml), anti-Axl (20 μg/ml), or IgG (20 μg/ml). Invasive properties were assessed by (*A–D*) scratch wound invasion and (*E–H*) chemotactic invasion

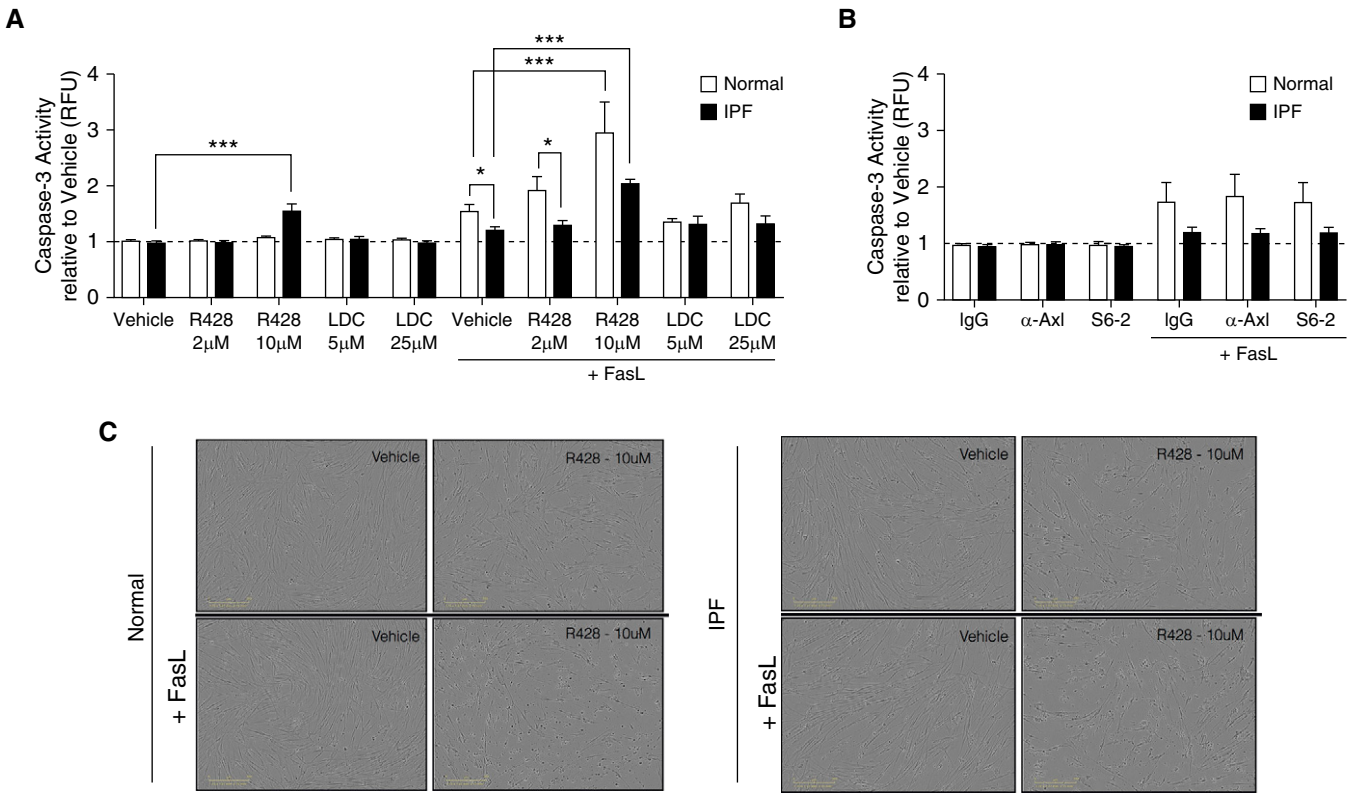

Figure 6. Proapoptotic and antiproliferative effects of TAM (Tyro3, Axl, and Mertk) receptor inhibitors in normal and IPF fibroblasts. (*A* and *B*) Fibroblast cultures derived from normal and IPF lungs were treated with the small-molecule inhibitors R428 (2 and 10 μM) and LDC (5 and 25 μM) or vehicle; and the antibodies S6 (4 μg/ml), anti-Axl (20 μg/ml), or IgG (20 μg/ml). Caspase-3 activity was evaluated after treatment with (*A*) small-molecule inhibitors or (*B*) the antibodies. FasL (75 ng/ml) plus His-Tag cross-linking antibody (5 μg/ml) was added to other cultures of fibroblasts for 18 hours. Data are mean ± SEM, $n = 3$–4 per group. $^{*}P \leq 0.05$, $^{***}P \leq 0.001$. (*C*) Representative images from normal and IPF fibroblasts treated with R428 (10 μM) or vehicle in the presence or absence of FasL for 18 hours. (*D*) Cell proliferation was assessed for 18 hours according to the percentage of cell confluence using IncuCyte ZOOM software. Data are representative findings from a normal and IPF fibroblast line that were tested under the conditions described previously. Data from additional normal ($n = 3$) and IPF ($n = 4$) fibroblast lines are shown in Figure E3. Scale bars in *C* are 300 μm. Data in *D* are mean ± SEM. α-Axl = anti-Axl; Axl = anexelekto; IPF = idiopathic pulmonary fibrosis; LDC = LDC1267; Mertk = MER proto-oncogene, tyrosine kinase; RFU = relative fluorescent units; Tyro3 = TYRO3 protein tyrosine kinase 3.

extent, R428 but not BIBF1120 (Figure 4D). In addition, R428 and, to a lesser extent, BIBF1120, but not LDC had significant inhibitory effects on collagen 1 protein expression at 24 and 72 hours in IPF fibroblasts with and without CpG compared with the appropriate vehicle control group (Figures 4E and 4F). In separate experiments, the effects of R428 were compared with those of S6 on αSMA and collagen 1 protein in normal and IPF fibroblasts activated with recombinant TGF-β. Although both R428 and S6 had no effect on reducing TGF-β–induced αSMA expression in both fibroblast types, R428 but not S6 significantly inhibited TGF-β–induced collagen expression in normal and IPF fibroblasts (*see* Figure E2A). Finally, R428, but not S6, reduced transcript expression for *COL1A1*, *COL3A1*, *FN1*, and *PDGFRA* in both normal and IPF fibroblasts at 7 days after vehicle, R428, or S6 treatment (*see* Figure E2B). Interestingly, R428 but not S6 treatment eliminated $SSEA4^{+}$ progenitor cells in these same normal and IPF fibroblast cultures (*see* Figure E2C). Thus, unlike LDC, BIBF1120, or S6 treatments, R428 had significant inhibitory effects on pAxl expression and collagen transcript and protein generation in IPF myofibroblasts.

R428 but Not Gas6- or Axl-Specific Antibodies Inhibit Invasiveness of IPF Fibroblasts

We next determined the effect of Gas6/TAM targeting approaches in functional assays with both normal and IPF

Figure 5. (Continued). for a minimum of 60 hours. Data are shown as a representative of normal ($n = 3$) and IPF fibroblast ($n = 3$) lines that were tested under similar conditions. Data are mean ± SEM. CC008-16, CC009-16, IPF02-16, IPF06-15, IPF09-14, and NLw2 are individual cell lines used in our experiments. αAxl = anti-Axl; Axl = anexelekto; BIBF = BIBF1120 (nintedanib); Gas6 = growth arrest–specific 6; IPF = idiopathic pulmonary fibrosis; LDC = LDC1267; Mertk = MER proto-oncogene, tyrosine kinase; Tyro3 = TYRO3 protein tyrosine kinase 3.

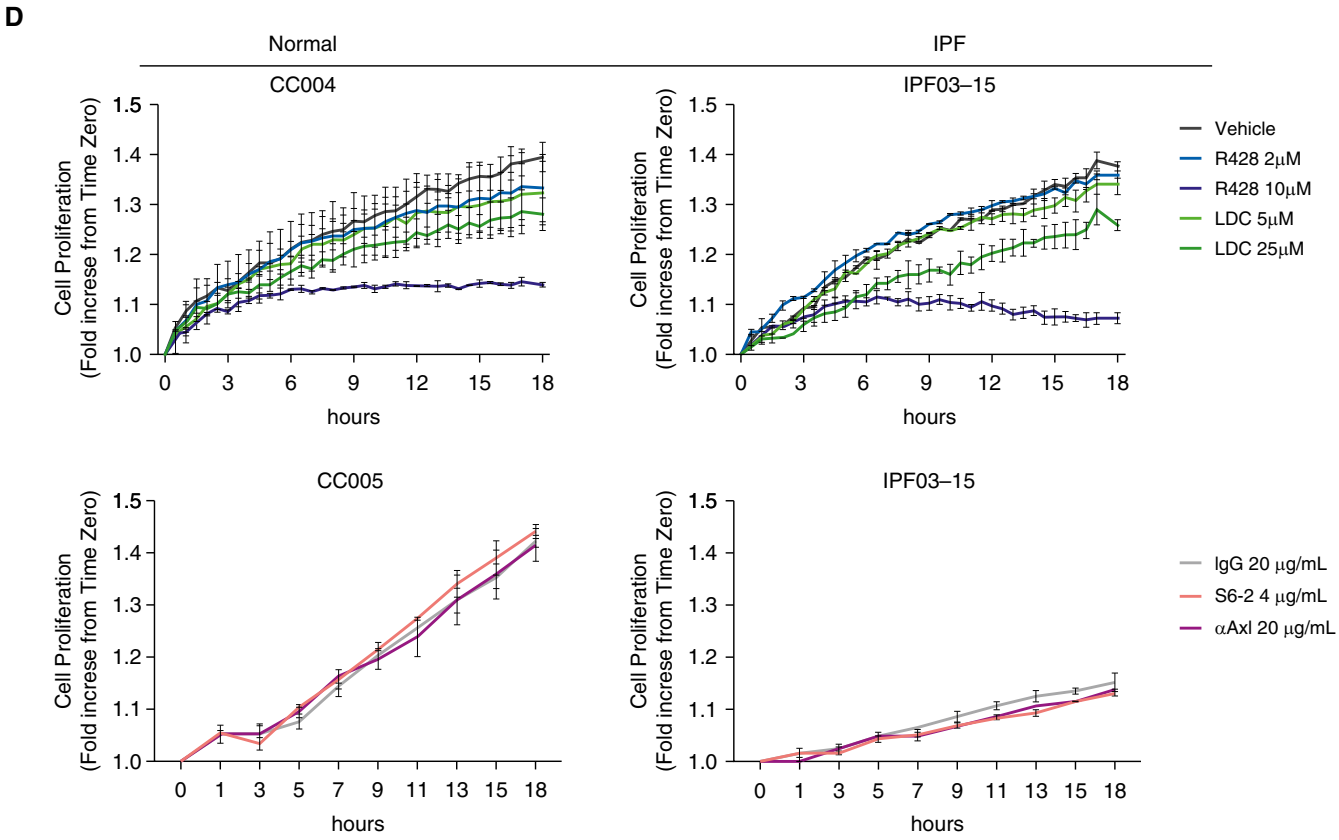

Figure 6. (Continued).

fibroblasts. As shown in Figure 5, the responses by normal and IPF fibroblast lines were determined in an invasive wound healing assay (Figures 5A–5D) and a chemotactic invasion assay (Figures 5E–5H). R428 was most effective at inhibiting invasive wound healing (Figures 5A and 5B) and chemotactic invasion (Figures 5E and 5F) of both normal and IPF fibroblasts. LDC was more effective than BIBF1120 at inhibiting normal and IPF fibroblast invasion in the invasive wound healing assay (Figures 5A and 5B), but both of these compounds showed similar efficacies in the chemotactic invasion of normal and IPF fibroblasts (Figures 5E and 5F). In contrast, S6 and anti-Axl mAb (11, 26, 27) did not alter the invasive properties of both normal (Figures 5C and 5G) and IPF fibroblast lines (Figures 5D and 5H). Thus, pharmacologic targeting of TAM receptors was more efficacious than biologic targeting of Gas6/Axl in functional assays of human lung fibroblasts.

R428 but Not Gas6- or Axl-Specific Antibodies Induce Apoptosis in IPF Fibroblasts

We next addressed whether R428 had proapoptotic effects in fibroblasts. R428 treatment at 10 μM alone significantly induced apoptosis in IPF fibroblasts, and this treatment enhanced FasL-induced apoptosis in both normal and IPF fibroblasts compared with the appropriate vehicle control group (Figure 6A). In contrast, the presence of IgG, anti-Axl mAb, or S6-2 did not modulate FasL-induced apoptosis in cultures of normal and IPF fibroblasts (Figure 6B). The effects of R428 compound ± FasL are shown in Figure 6C, where it was evident that the number of apoptotic bodies was increased in compound-treated and compound + FasL-treated normal (left panels) and IPF (right panels) fibroblast. In representative normal and IPF fibroblast lines, the antiproliferative effect of both R428 and LDC on these cells was apparent (Figure 6D, top panels) but neither the anti-Axl mAb or S6-2 had any effect on fibroblast proliferation compared with the appropriate IgG control group (Figure 6D, bottom panels). Not all fibroblast lines proliferated over the time examined but R428 consistently reduced the numbers of normal (*see* Figure E3A) and IPF (*see* Figure E3B) nonproliferating fibroblasts in culture, presumably because of the proapoptotic effects of this compound (*see* Figure E3). Together, these data demonstrate that R428 promoted apoptosis and inhibited proliferation in human lung fibroblasts.

Gas6/TAM Receptors Promote and Exacerbate Experimental Pulmonary Fibrosis

The *in vivo* role of Gas6/TAM receptors was next addressed using two experimental models of pulmonary fibrosis. In a humanized SCID/Bg model (Figure 7A), both Gas6 and Axl transcripts are significantly increased in the lungs at Days 21 and 35 after IPF fibroblast injection compared

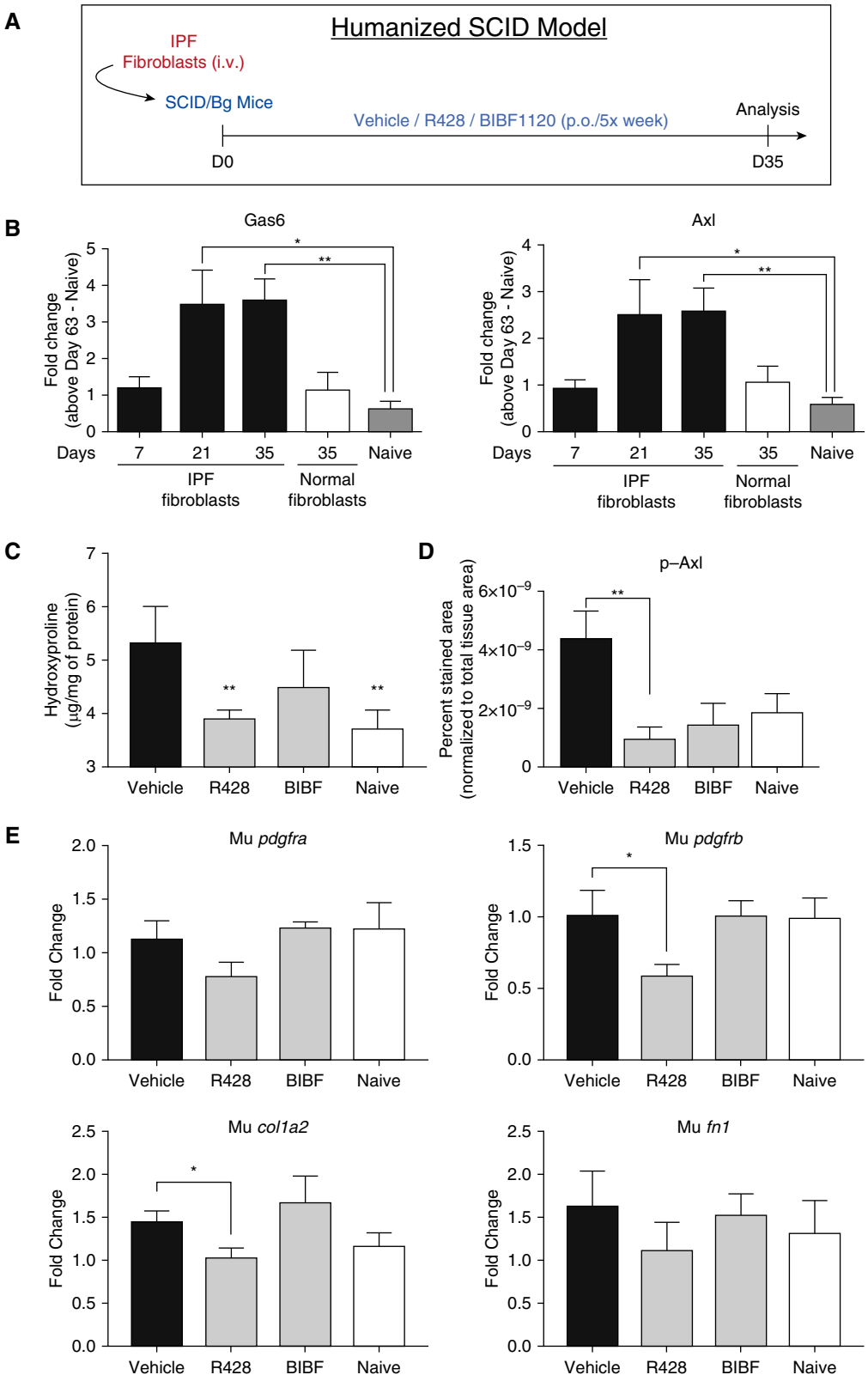

Figure 7. Role of Gas6/TAM (Tyro3, Axl, and Mertk) receptor activation in experimental pulmonary fibrosis. Treatment protocol is as follows: humanized SCID/Bg mice were injected with idiopathic pulmonary fibrosis fibroblasts and subsequently treated orally with R428 (5 mg/kg), BIBF1120 (30 mg/kg), or the appropriate vehicle. (*A*) Treatments were given from Day 0 to Day 35 after fibroblast injection, and lungs were analyzed at Day 35. (*B*) Gas6 and Axl gene expression in lungs of other groups of SCID/Bg mice that received either idiopathic pulmonary fibrosis or normal fibroblasts by intravenous injection

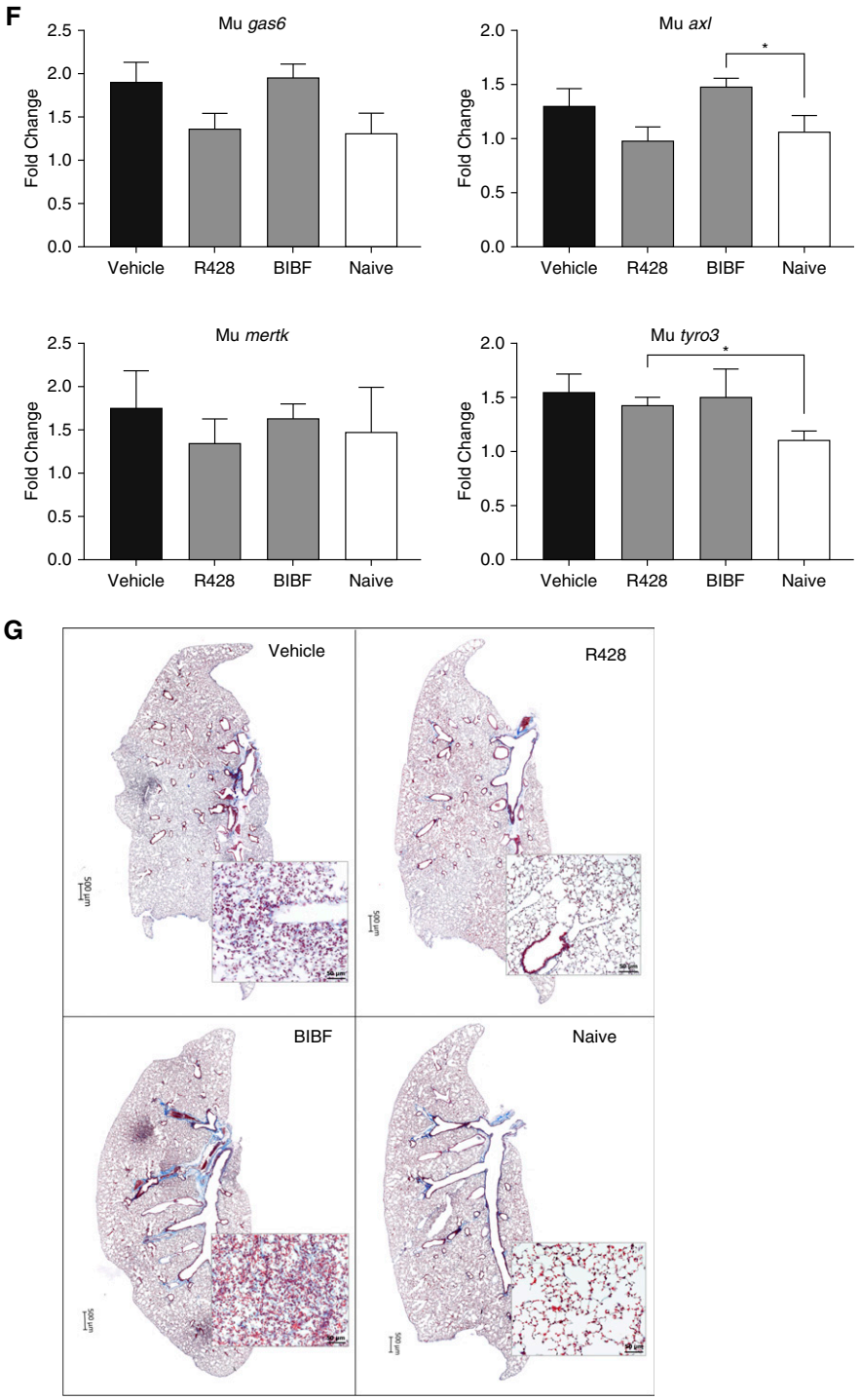

Figure 7. (Continued). and unchallenged mice (naive), and transcripts were evaluated at Days 7, 21, and 35 after injection. (*C–F*) The following analyses at Day 35 after treatments in humanized SCID/Bg mice are shown: hydroxyproline levels (*C*), p-Axl quantification (*D*), transcript expression of murine *PDGFRα*, *PDGFRβ*, *Col1a2*, *FN1* (*E*), and transcript expression of *Gas6*, *Axl*, *Mertk*, and *Tyro3* (*F*). (*G*) Representative images of Masson trichrome staining in whole lungs and affected areas (see insets). Whole-lung p-Axl was determined using a PathScan phospho-Axl (panTyr) sandwich ELISA kit. Data are mean ± SEM, $n = 3–5$ per group. $^{*}P \leq 0.05$; $^{**}P \leq 0.01$. $^{**}P$ is compared with the vehicle group. Axl = anexelekto; BIBF = BIBF1120 (nintedanib); *col1a2* = collagen 1 α 2; D = day; *fn1* = fibronectin 1; Gas6 = growth arrest–specific 6; IPF = idiopathic pulmonary fibrosis; Mertk = MER proto-oncogene, tyrosine kinase; Mu = *Mus musculus*; p-Axl = phosphorylated Axl; p.o. = per os (oral gavage); *pdgfr* = platelet-derived growth factor receptor; Tyro3 = TYRO3 protein tyrosine kinase 3.

with normal fibroblasts injected and nonhumanized, naive, SCID/Bg mouse lungs (Figure 7B); the later time point coincides with the histologic appearance of fibrosis in this model (28). To determine the role of TAM receptors in this model, vehicle, R428, or BIBF1120 were administered from Days 0 to 35 after IPF fibroblast injection and ensuing remodeling in the small molecule–treated groups was compared with the vehicle group (Figure 7A). R428 but not BIBF1120 significantly decreased hydroxyproline content in the mouse lungs (Figure 7C). Whole-lung pAxl was also significantly reduced in the R428-treated mice (Figure 7D). Reduced transcript levels for mouse *pdgfrb* and *col1a2* were also observed in lungs of humanized SCID/Bg mice treated with R428 (Figure 7E), but no difference was observed for mouse *pdgfra* and *fn1* (Figure 7E) or *gas6*, *axl*, *mertk*, and *tyro3* transcripts (Figure 7F) in the treated groups compared with vehicle. Histologically, representative lung sections from the R428-treated group of humanized SCID/Bg mice were similar to the naive SCID/Bg group (Figure 7G, right panels). In contrast, BIBF1120-treated humanized SCID/Bg mice exhibited lung fibrosis that was similar to that in the vehicle-treated humanized SCID/Bg group (Figure 7G, left panels).

None of the treatments altered free Gas6 levels in BAL and serum from humanized SCID/Bg mice (*see* Figure E4A) but both R428 and BIBF1120 significantly reduced Tyro3 expression compared with humanized SCID/Bg mice that received vehicle (*see* Figure E4B). Neither treatment altered mouse inflammatory genes associated with fibrosis including *nos2*, *tnf*, *il6*, and *ptgs2* (*see* Figure E4C). In a bleomycin-induced pulmonary fibrosis model (*see* Figure E4D), transcript levels for *axl*, *mertk*, and *gas6* but not *tyro3* were all significantly elevated at Day 14 after bleomycin compared with the saline controls (*see* Figure E4E), suggesting that TAM pathway is activated in this model. Furthermore, $Gas6^{-/-}$ mice had significantly less hydroxyproline compared with wild-type, $Gas6^{+/+}$, mice at Day 14 after bleomycin (*see* Figure E4F). Thus, these data demonstrated that Gas6/TAM receptors contributed to the development of pulmonary fibrosis in two experimental models.

Discussion

A key component of fibrosis in IPF involves the aberrant conversion of fibroblasts into myofibroblasts and the persistence of these myofibroblasts. This disease is also associated with considerable mesenchymal expansion within the lung and increased invasiveness of these mesenchymal cells (29). Using both genome-wide and proteomic analyses of lung samples and functional assays of primary human fibroblasts derived from the same lung samples, we explored the expression and role of Gas6 and TAM receptors in IPF. In the present study, it was apparent that the Gas6/Axl/Tyro3 pathway was increased and active, both in lung tissues and in cultured fibroblasts and mesenchymal progenitor cells (21) from these same lung tissues.

Although our transcript analysis did not reveal increased expression for Tyro3 and Mertk in IPF tissues and cells compared with normal tissues and cells, our protein analyses showed that Tyro3 (but not Mertk) was expressed at the protein level in both IPF tissues and primary lung fibroblasts. Targeting this pathway with a soluble Axl decoy receptor modulated IPF fibroblast to myofibroblast activation but this Axl-targeted antibody was less effective in modulating IPF fibroblast function compared with small-molecule inhibitors that more generally targeted the TAM receptors' kinase activity. One caveat to the use of small-molecule TAM receptor inhibitors in the current study is that all have off-target effects that might impact critical antifibrotic pathways beyond the TAM pathway. Notwithstanding, R428 inhibited fibroblast invasion, CpG- and TGF-β–induced fibroblast synthetic activity, and markedly modulated both apoptosis and proliferation in these cells. R428 has been shown to have inhibitory effects on Tie-2 (TEK receptor tyrosine kinase 2), Ftl-1 (Fms-like tyrosine kinase-1), Flt-3 (Fms-like tyrosine kinase-3), Ret (Ret proto-oncogene), and Abl (Abl tyrosine kinase) (25), but none of these kinases are widely recognized as mediators of pulmonary fibrosis. At higher concentrations, R428 has inhibitory effects on the insulin receptor and VEGFR2 (vascular endothelial growth factor receptor 2) (25), but ongoing studies in our laboratory with more specific inhibitors of these RTKs suggest that neither of these receptors have major roles in the development or exacerbation of pulmonary fibrosis. The expression of Tyro3 by IPF fibroblasts might explain the variable effects of the various Gas6/TAM receptor targeting agents on these cells because targeting the Axl receptor alone was not sufficient to fully inhibit both their synthetic and functional properties. Furthermore, R428, and to a lesser extent S6, significantly decreased pAxl protein over 24 hours in a dose-dependent manner and the former was clearly the more effective Gas6/TAM receptor targeting agent in IPF fibroblasts. Although BIBF1120 targets numerous RTKs, there was no prior evidence that this drug targets the Gas6/TAM receptor pathway (2). Our *in vitro* analysis revealed that 300 nM of BIBF1120 significantly inhibited IPF fibroblast invasion, myofibroblast differentiation, and total Axl expression but this drug had modest effects on other properties of fibroblasts including proliferation, apoptosis, and free Gas6 levels compared with the TAM receptor inhibitor.

In two experimental fibrosis models, the Gas6/TAM receptor pathway was both increased and active, and the targeting of this pathway via R428 treatment or Gas6 gene deletion attenuated pulmonary fibrosis. Although targeting TAM receptors with R428 did not alter Gas6 levels in humanized SCID/Bg mouse model of pulmonary fibrosis, pAxl and Tyro3 proteins and the magnitude of lung remodeling were significantly reduced compared with vehicle-treated humanized SCID/Bg mice. Thus, the profibrotic effects of Gas6 seem to be mediated via both Axl and Tyro3 receptors in IPF. BIBF1120 at 30 mg/kg daily dosing regimen has been shown previously to inhibit the development of pulmonary fibrosis in a bleomycin-induced pulmonary fibrosis model (30); but BIBF1120 delivered at this daily dose had a partial effect on pulmonary fibrosis despite its reduction of both human pAxl and Tyro3 proteins in a humanized SCID/Bg model. Given our observed antiproliferative and proapoptotic effect of R428, but not BIBF1120, on IPF lung fibroblasts, one explanation for the *in vivo* findings is the persistence of the human IPF fibroblasts in humanized mice following BIBF1120 but not R428 therapy. In addition, both mouse *gas6* and *axl* transcripts were increased in humanized SCID/bg mice compared with naive SCID/bg mice, and

R428 but not BIBF1120 treatment reduced their levels to naive baseline. Together, these data demonstrate that targeting Gas6/TAM receptors in fibroblast (and possibly in putative fibroblast progenitors [22]) might be a therapeutic strategy in IPF.

In conclusion, Gas6/TAM receptor activation contributes to fibrosis in IPF. Although the focus of the present study was to elucidate the role of this pathway in mesenchymal cells, other nonimmune and immune cells showed evidence of increased Axl activation. Given recent findings that Axl is activated in hyperplastic IPF epithelial cells and might contribute to the loss of the epithelial integrity in this disease (31), further studies are warranted in other IPF cells. At present, future studies directed at targeting this pathway in clinical trials warrant consideration. ■

Author disclosures are available with the text of this article at www.atsjournals.org.

References

1. Blackwell TS, Tager AM, Borok Z, Moore BB, Schwartz DA, Anstrom KJ, *et al*. Future directions in idiopathic pulmonary fibrosis research. An NHLBI workshop report. *Am J Respir Crit Care Med* 2014;189: 214–222.
2. Richeldi L, du Bois RM, Raghu G, Azuma A, Brown KK, Costabel U, *et al*.; INPULSIS Trial Investigators. Efficacy and safety of nintedanib in idiopathic pulmonary fibrosis. *N Engl J Med* 2014;370: 2071–2082.
3. Richeldi L, Cottin V, du Bois RM, Selman M, Kimura T, Bailes Z, *et al*. Nintedanib in patients with idiopathic pulmonary fibrosis: combined evidence from the TOMORROW and INPULSIS(®) trials. *Respir Med* 2016;113:74–79.
4. Bellido-Martín L, de Frutos PG. Vitamin K-dependent actions of Gas6. *Vitam Horm* 2008;78:185–209.
5. Axelrod H, Pienta KJ. Axl as a mediator of cellular growth and survival. *Oncotarget* 2014;5:8818–8852.
6. Korshunov VA. Axl-dependent signalling: a clinical update. *Clin Sci (Lond)* 2012;122:361–368.
7. Hafizi S, Dahlbäck B. Signalling and functional diversity within the Axl subfamily of receptor tyrosine kinases. *Cytokine Growth Factor Rev* 2006;17:295–304.
8. Gerloff J, Korshunov VA. Immune modulation of vascular resident cells by Axl orchestrates carotid intima-media thickening. *Am J Pathol* 2012;180:2134–2143.
9. Melaragno MG, Wuthrich DA, Poppa V, Gill D, Lindner V, Berk BC, *et al*. Increased expression of Axl tyrosine kinase after vascular injury and regulation by G protein-coupled receptor agonists in rats. *Circ Res* 1998;83:697–704.
10. Bauer T, Zagórska A, Jurkin J, Yasmin N, Köffel R, Richter S, *et al*. Identification of Axl as a downstream effector of TGF-β1 during Langerhans cell differentiation and epidermal homeostasis. *J Exp Med* 2012;209:2033–2047.
11. Shibata T, Habiel DM, Coelho AL, Kunkel SL, Lukacs NW, Hogaboam CM. Axl receptor blockade ameliorates pulmonary pathology resulting from primary viral infection and viral exacerbation of asthma. *J Immunol* 2014;192:3569–3581.
12. Shibata T, Ismailoglu UB, Kittan NA, Moreira AP, Coelho AL, Chupp GL, *et al*. Role of Gas6 in the development of fungal allergic airway disease in mice. *Am J Respir Cell Mol Biol* 2014;51: 615–625.
13. Fourcot A, Couchie D, Chobert MN, Zafrani ES, Mavier P, Laperche Y, *et al*. Gas6 deficiency prevents liver inflammation, steatohepatitis, and fibrosis in mice. *Am J Physiol Gastrointest Liver Physiol* 2011; 300:G1043–G1053.
14. Bellan M, Pogliani G, Marconi C, Minisini R, Franzosi L, Alciato F, *et al*. Gas6 as a putative noninvasive biomarker of hepatic fibrosis. *Biomarkers Med* 2016;10:1241–1249.
15. Bárcena C, Stefanovic M, Tutusaus A, Joannas L, Menéndez A, García-Ruiz C, *et al*. Gas6/Axl pathway is activated in chronic liver disease and its targeting reduces fibrosis via hepatic stellate cell inactivation. *J Hepatol* 2015;63:670–678.
16. Marí M, Tutusaus A, García de Frutos P, Morales A. Genetic and clinical data reinforce the role of GAS6 and TAM receptors in liver fibrosis. *J Hepatol* 2016;64:983–984.
17. Petta S, Valenti L, Marra F, Grimaudo S, Tripodo C, Bugianesi E, *et al*. MERTK rs4374383 polymorphism affects the severity of fibrosis in non-alcoholic fatty liver disease. *J Hepatol* 2016;64:682–690.
18. Salisbury ML, Xia M, Murray S, Bartholmai BJ, Kazerooni EA, Meldrum CA, *et al*. Predictors of idiopathic pulmonary fibrosis in absence of radiologic honeycombing: a cross sectional analysis in ILD patients undergoing lung tissue sampling. *Respir Med* 2016;118: 88–95.
19. Trujillo G, Meneghin A, Flaherty KR, Sholl LM, Myers JL, Kazerooni EA, *et al*. TLR9 differentiates rapidly from slowly progressing forms of idiopathic pulmonary fibrosis. *Sci Transl Med* 2010;2:57ra82.
20. Angelillo-Scherrer A, Burnier L, Lambrechts D, Fish RJ, Tjwa M, Plaisance S, *et al*. Role of Gas6 in erythropoiesis and anemia in mice. *J Clin Invest* 2008;118:583–596.
21. Xia H, Bodempudi V, Benyumov A, Hergert P, Tank D, Herrera J, *et al*. Identification of a cell-of-origin for fibroblasts comprising the fibrotic reticulum in idiopathic pulmonary fibrosis. *Am J Pathol* 2014;184: 1369–1383.
22. Xia H, Gilbertsen A, Herrera J, Racila E, Smith K, Peterson M, *et al*. Calcium-binding protein S100A4 confers mesenchymal progenitor cell fibrogenicity in idiopathic pulmonary fibrosis. *J Clin Invest* 2017; 127:2586–2597.
23. Kariolis MS, Miao YR, Jones DS II, Kapur S, Mathews II, Giaccia AJ, *et al*. An engineered Axl 'decoy receptor' effectively silences the Gas6-Axl signaling axis. *Nat Chem Biol* 2014;10:977–983.
24. Meneghin A, Choi ES, Evanoff HL, Kunkel SL, Martinez FJ, Flaherty KR, *et al*. TLR9 is expressed in idiopathic interstitial pneumonia and its activation promotes in vitro myofibroblast differentiation. *Histochem Cell Biol* 2008;130:979–992.
25. Holland SJ, Pan A, Franci C, Hu Y, Chang B, Li W, *et al*. R428, a selective small molecule inhibitor of Axl kinase, blocks tumor spread and prolongs survival in models of metastatic breast cancer. *Cancer Res* 2010;70:1544–1554.
26. Ye X, Li Y, Stawicki S, Couto S, Eastham-Anderson J, Kallop D, *et al*. An anti-Axl monoclonal antibody attenuates xenograft tumor growth and enhances the effect of multiple anticancer therapies. *Oncogene* 2010;29:5254–5264.
27. Shibata T, Ismailoglu UB, Kittan NA, Moreira AP, Coelho AL, Chupp GL, *et al*. Role of growth arrest-specific gene 6 in the development of fungal allergic airway disease in mice. *Am J Respir Cell Mol Biol* 2014;51:615–625.
28. Pierce EM, Carpenter K, Jakubzick C, Kunkel SL, Flaherty KR, Martinez FJ, *et al*. Therapeutic targeting of CC ligand 21 or CC chemokine receptor 7 abrogates pulmonary fibrosis induced by the adoptive transfer of human pulmonary fibroblasts to immunodeficient mice. *Am J Pathol* 2007;170:1152–1164.
29. Noble PW, Barkauskas CE, Jiang D. Pulmonary fibrosis: patterns and perpetrators. *J Clin Invest* 2012;122:2756–2762.
30. Wollin L, Maillet I, Quesniaux V, Holweg A, Ryffel B. Antifibrotic and anti-inflammatory activity of the tyrosine kinase inhibitor nintedanib in experimental models of lung fibrosis. *J Pharmacol Exp Ther* 2014; 349:209–220.
31. Fujino N, Kubo H, Maciewicz RA. Phenotypic screening identifies Axl kinase as a negative regulator of an alveolar epithelial cell phenotype. *Lab Invest* 2017;97:1047–1062.